

# Assessing Radiological Risks and Natural Radioactivity in Building Materials from Ica, Peru

Félix Díaz<sup>1</sup>, Rafael Liza<sup>2</sup>, Nhell Cerna<sup>3</sup>, Patrizia Pereyra<sup>4</sup>, Daniel Palacios<sup>4</sup>, Jhonny Rojas<sup>4</sup>, Laszlo Sajó<sup>5</sup>

<sup>1</sup>Vicerrectorado de Investigación, Universidad Autónoma del Perú, Perú, [fediazdes@autonoma.edu.pe](mailto:fediazdes@autonoma.edu.pe)

<sup>2</sup>Universidad Tecnológica del Perú, Perú, [c20231@utp.edu.pe](mailto:c20231@utp.edu.pe)

<sup>3</sup>Universidad Privada del Norte, Perú, [nhell.cerna@upn.pe](mailto:nhell.cerna@upn.pe)

<sup>4</sup>Pontificia Universidad Católica del Perú, Perú, [ppereyr@pucp.edu.pe](mailto:ppereyr@pucp.edu.pe), [dpalaciosf@pucp.edu.pe](mailto:dpalaciosf@pucp.edu.pe), [irojash@pucp.edu.pe](mailto:irojash@pucp.edu.pe)

<sup>5</sup>Alba Regia Technical Faculty, Óbuda University, Hungary, [sajo@usb.v](mailto:sajo@usb.v)

**Abstract**– *The study investigated the radon emission rate and potential radiological hazards of high-uranium-content building materials in The Ica area of Southwestern Peru. We used a creative technique that combined a closed chamber and active monitor, and it was improved by a hermetic sealing method to maintain secular equilibrium well. The results showed radon emission rates as low as below detection limits (BDL) up to 52.3 mBq/kg-h. Our analyses with a 3' x 3' NaI detector found radionuclide concentrations in cement samples by gamma spectrometry. We found a high positive correlation between radium activity concentration and radon exhalation rate. The activity concentrations of <sup>226</sup>Ra, <sup>232</sup>Th, and <sup>40</sup>K differ significantly, with maximum values reaching 60.6, 22.3, and 1074 mBq/kg-h. We consider these results significant for the safety of materials in the Peruvian construction sector. And we also hope that they will provide information to support radiological risk management.*

**Keywords**–*Building Materials, Radiological Risks, Radionuclides.*

## I. INTRODUCTION

Radioactive isotopes can be found in soil, rocks, and construction materials, pointing to significant environmental radiation sources and health implications [1]. Environmental radiation consists of natural internal exposure due mainly to inhaling radon daughters or other particles (NORM) and external exposure from gamma rays emitted naturally by radioactive materials [2]. The external exposure, which affects both indoor and outdoor environments, can, for the most part, be attributed to gamma rays emitted by isotopes like <sup>40</sup>K, as well as intermediary decay products from the longer-lived isotopes <sup>226</sup>Ra (<sup>238</sup>U) and <sup>232</sup>Th series [3]. Health risk assessments require a comprehensive understanding of the many sources and types of radiation associated with this radiation exposure.

The production of building materials necessitates extracting raw materials from quarries, leading to variations in activity concentrations of materials like bricks, cement, and gypsum [4]. Ionizing radiation, known to cause molecular damage in living tissues, is quantified by the effective dose, reflecting radiation type and tissue sensitivity. This metric represents the overall risk associated with ionizing radiation exposure, significantly influenced by radioactive elements in construction materials. The impact of these materials on indoor radiation levels poses a health risk, contingent on factors such as material composition, local geology, and

architectural design. Since 77% of the population of Peru resides in urban settings, spending considerable time indoors, evaluating the radiation from building materials becomes crucial for estimating potential risks to inhabitants. In Peru, where regulation is guided by international recommendations, monitoring and managing radionuclide activity in building materials is vital. Such oversight is crucial to determine the health risk increase from long-term exposure to elevated radiation dose rates.

The UNSCEAR 2000 report elucidates that radon and its decay products collectively contribute to an average inhaled dose of 1.26 mSv/y, constituting approximately half of the annual effective dose (2.4 mSv/y) received by individuals from natural sources [5-7]. Notably, the International Commission on Radiological Protection (ICRP) and the World Health Organization (WHO) acknowledge the challenges of radon and external irradiation from building materials as critical public health concerns.

Radon gas, predominantly accumulating in poorly ventilated spaces like homes, is a primary determinant of indoor radon levels [8]. This accumulation stems from radon exhalation, a process initiated by radon emanation. Radon emanation refers to releasing radon atoms from the internal structure of materials, such as soils and building materials, into their pores [9]. The radon exhalation rate from these materials is influenced by intrinsic factors, such as radium content and physical properties, and extrinsic factors, including air pressure, temperature, and relative humidity [10]. Measuring the radon exhalation rate from building materials is imperative for assessing radiological risk levels.

Effective risk management includes ensuring adequate ventilation and conducting air quality assessments, which are essential for residential spaces' safety and regulatory adherence. Additionally, evaluating the radon exhalation rate in existing structures is crucial for devising appropriate mitigation strategies, particularly when radon levels exceed national regulatory thresholds. In Peru, research on radon exposure has gained significant interest recently, with studies such as [11,12]. However, regulations that limit the dose of exposure to construction materials have yet to be established due to the wait for new research that provides a more significant amount of data from different regions of the country and all types of construction materials.

This study aims to evaluate the concentration of natural radioactivity, the radon exhalation rate, and the radiological risk indexes (Gamma index, Radium equivalent activity, External hazard index, Internal hazard index) of the most common construction materials in Ica, Peru. With this study, we hope to inform public policy, improve building practices, and increase public awareness of the impact of building materials on radon exposure. This advice should regulate and establish safe limits for radionuclides in building materials for efficient supervision and control. Additionally, the effectiveness of one method with three different settings for hermetically sealing the container used in gamma-ray spectrometry was also studied.

## II. MATERIALS AND METHODS

### A. Sample collection and preparation

Fourteen building material samples were collected from Ica, a coastal city in Peru, for analytical purposes. To prepare these samples for analysis, they were dried at 110 °C for 24 hours, a step crucial for removing moisture. Subsequently, the dried samples were pulverized and sieved to achieve a uniform particle size of 1 mm. This preparation was essential for accurate gamma radiation measurements and determining the radon mass exhalation rate.

The samples comprised cement and bricks procured from principal manufacturing facilities along the Peruvian coast. Additionally, aggregates used in concrete (such as sand and rock) and gypsum samples were specifically sourced from areas within the Ica region. These locations were chosen due to their proximity to zones with notable anomalies in uranium concentration, as reported in previous studies [13]. Figure 1 in the study provides a detailed illustration of the extraction sites for gypsum and aggregates, with areas denoted by red circles highlighting regions of potential uranium mining interest.

### B. Measurement of natural radioactivity

Samples of building materials sourced from diverse manufacturers were collected and processed. Post-processing, these samples were stored in high-density polyethylene containers equipped with screw caps. The specifications of these containers are as follows: an external diameter of 85.4 mm, a filling height of 139.98 mm, a side thickness of 1.96 mm, and a base thickness of 2.20 mm.

A leak test validated the radon impermeability of the cylindrical plastic containers designated for gamma spectrometry analyses. This test employed the AlphaGuard (AG) equipment, configured in diffusion mode, as a radon monitoring apparatus. The procedure was carried out within a methacrylate accumulation chamber, as illustrated in Figure 2D. A uranium ore sample was positioned inside the cylindrical container for this purpose. Additionally, the efficacy of three distinct sealing methodologies applied to the container was evaluated, as depicted in Figure 2.

**Digital Object Identifier:** (only for full papers, inserted by LACCEI).  
**ISSN, ISBN:** (to be inserted by LACCEI).  
**DO NOT REMOVE**

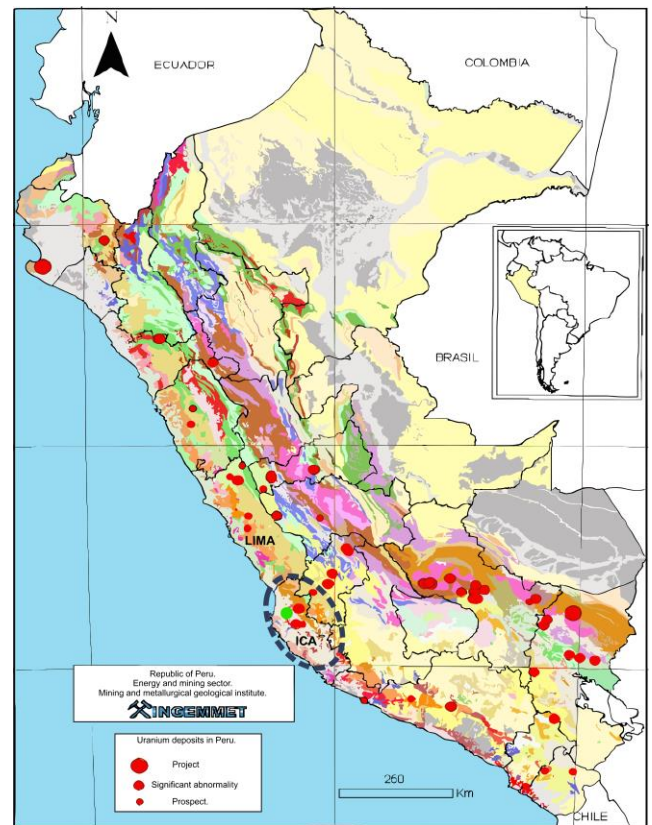


Fig. 1 The enclosed area delineated by the dotted blue line represents the region from which natural mineral materials utilized as primary raw materials in the construction products examined in this study are extracted. The marked green point identifies the principal extraction site for raw materials used in brick production. This site is situated on the central coast of Peru, specifically southwest of Lima, in the Ica department [13].

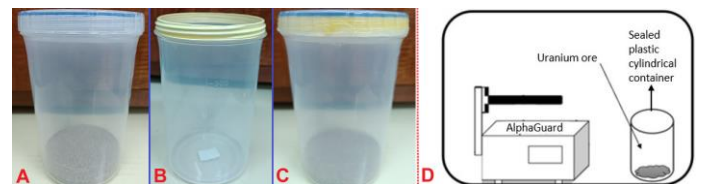


Fig. 2 The experimental setup for evaluating sealing methods and assessing leakage is illustrated. On the left side, three distinct sealing techniques are depicted: Figure 2A demonstrates the method of fully tightening the screw cap, Figure 2B exhibits the application of Teflon tape on the thread, and Figure 2C illustrates the process of applying high-vacuum grease to the internal contour of the screw cap, in conjunction with covering the thread with Teflon tape. On the right side, Figure 2D presents the configuration within the accumulation chamber, specifically designed to measure container leakage.

Subsequently, the containers were sealed employing a technique that effectively minimized radon leakage, thus ensuring the maintenance of secular equilibrium between  $^{226}\text{Ra}$ ,  $^{222}\text{Rn}$ , and their short-lived progeny. Once secular equilibrium was established, the samples underwent analysis using a gamma spectrometer equipped with a 3" x 3" NaI(Tl)

scintillation detector. This detector boasted a resolution of less than or equal to 8.5% at the 662 keV peaks of  $^{137}\text{Cs}$ . In order to standardize measurements, the cylindrical plastic containers housing the building materials were placed on a support made of low-density plastic. The identification of natural radionuclides such as  $^{40}\text{K}$ ,  $^{226}\text{Ra}$ , and  $^{232}\text{Th}$  was facilitated through the observation of their respective energy peaks, as delineated in Figure 3.

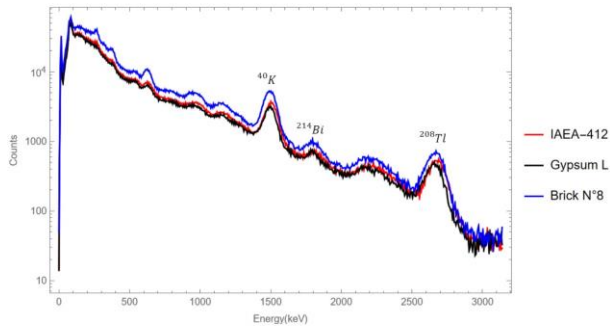


Fig. 3 Gamma spectral analysis of diverse materials including Gypsum, Brick, and the IAEA reference sample.

Gamma spectral measurements for the background, various samples, and reference material were conducted over 86400 seconds. During the analysis, full energy peaks were identified, regions of interest (ROI) were established, and the net areas of the peaks were calculated using the MAESTRO®-32 MCA Emulation software. The system's minimum detectable activity (MDA) was calculated with a 95% confidence level. Typically, energy calibration in such analyses is conducted using point sources, and efficiency calibration is executed with reference materials. However, in this particular study, energy calibration was considered non-essential due to the radionuclide similarities between the building material samples and the IAEA-412 (Ocean Sediment) reference material.

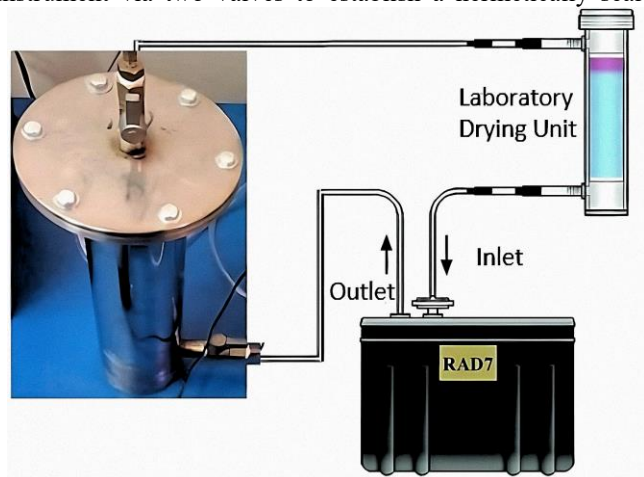
The Extended Relative Method of Activity Determination (ERMAD) was utilized to quantify activity. Notwithstanding the consistent use of cylindrical geometry, variations were observed in the sizes of containers and the volumes occupied by the samples and reference material. The ETNA software was employed to estimate the efficiency transfer factor required for the ERMAD process to accommodate these variations.

### C. Measurement of radon mass exhalation rates

The assessment of radon exhalation from the surface area of granular materials such as soil, rock, or building materials presents a considerable challenge owing to the myriad factors that influence this process. Determining this parameter necessitates an integrated approach combining experimental methodologies with theoretical modeling to yield reliable and

significant outcomes. The granular nature of these materials implies that the total surface area contributing to radon exhalation extends beyond the external surface to encompass the surfaces of each particle. This complexity is further amplified by the variability in grain size, shape, and radon content, as well as the presence of intergranular voids, making the measurement process more intricate. Consequently, it is a standard practice in such contexts to quantify the radon exhalation rate about mass [14,15].

For this purpose, a specially designed cylindrical stainless steel accumulation chamber was utilized. This chamber, characterized by a negligible radon leakage rate as corroborated in [12], was integrated with the RAD7 instrument via two valves to establish a hermetically sealed



circuit, as depicted in Figure 4.

Fig. 4 Experimental Configuration for Radon Exhalation: The RAD7 instrument measured the radon exhalation rate from a sample housed within the stainless-steel accumulation chamber.

The radon concentration within the stainless-steel accumulation chamber, represented as  $C(t)$ , is governed by the ensuing radon mass transfer equation, as delineated in the study by [16].

$$\frac{dC(t)}{dt} = \frac{E(t)S}{V_c} - \lambda_{Rn}C - \lambda_L C - \lambda_{BD}C. \quad (1)$$

In the context of radon exhalation measurement, ' $E$ ' denotes the radon exhalation rate, ' $S$ ' signifies the surface area from which radon exhalates, and ' $V_c$ ' represents the total volume within the enclosed chamber, inclusive of the volume occupied by the RAD7 measurement mechanism. Additionally, the term ' $\lambda_{BD}$ ' corresponds to the rate of back-diffusion, ' $\lambda_L$ ' defines the rate of radon leakage, and ' $\lambda_{Rn}$ ' denotes the radon decay constant.

For brief sampling durations, specifically during the initial 24 hours wherein a linear increase in radon concentration predominantly characterizes the accumulation process within the sealed chamber [17,18], it is feasible to consider both the

back-diffusion rate ' $\lambda_{BD}$ ' and the radon leak rate ' $\lambda_L$ ' as negligible [19].

$$E_M = (m + \lambda_{Rn} C_0) \frac{V_c}{M} . \quad (2)$$

In this context, the unit (Bq.m<sup>-3</sup>.h<sup>-1</sup>) represents the initial rate of increase in radon concentration within the accumulation chamber. ' $M$ ' signifies the mass of the sample under examination.

The term "emanation fraction" pertains to the ratio of <sup>222</sup>Rn atoms produced within the grains of the materials that effectively migrate out of the pore space. Determining the radon emanation fraction can be conducted according to the methodologies outlined in [20].

$$f = \frac{E_M}{C_{Ra} \lambda_{Rn}} . \quad (3)$$

In the given expression,  $f$  denotes the radon emanation fraction,  $E_M$  represents the radon mass exhalation rate, expressed in units of (Bq.kg<sup>-1</sup>.h<sup>-1</sup>), and  $C_{Ra}$  refers to the concentration of <sup>226</sup>Ra, quantified in (Bq.kg<sup>-1</sup>).

#### D. Radiological parameters

Key radiological parameters were calculated to evaluate radiation hazards related to the building materials utilized. These include the Gamma index ( $I_\lambda$ ), the Radium equivalent activity ( $Ra_{eq}$ ), and both the External and Internal hazard indices ( $H_{ex}$ ,  $H_{in}$ ).

#### E. Gamma Index $I_\lambda$

The European Commission [21], along with various scholars [20,22], have recommended specific indices to evaluate the surplus gamma radiation emanating from building materials and its correlation with the annual dose rate. In this context, the Gamma index represents the cumulative impact of three radioisotopes commonly found in building materials <sup>226</sup>Ra, <sup>232</sup>Th, and <sup>40</sup>K. The following equation executes the calculation of the Gamma index:

$$I_\lambda = \frac{C_{226Ra}}{300} + \frac{C_{232Th}}{200} + \frac{C_{40K}}{3000} . \quad (4)$$

Building materials exhibiting a gamma index of 1 or higher possess the potential to yield annual effective doses surpassing 1 mSv. Conversely, materials with a gamma index value below 1 are considered safe for utilization per the guidelines established in [21].

#### F. Radium equivalent activity $Ra_{eq}$

The Radium Equivalent Activity ( $Ra_{eq}$ ) is a widely recognized index that quantifies a weighted sum of the activities of <sup>226</sup>Ra, <sup>232</sup>Th, and <sup>40</sup>K present in building materials. This index is formulated based on the methodology provided in [23].

$$Ra_{eq} = C_{Ra} + 1.43C_{Th} + 0.077C_K . \quad (5)$$

The maximum allowable dose rate for any building material is set at 1 mSv.y<sup>-1</sup>, which corresponds to a Radium Equivalent Activity ( $Ra_{eq}$ ) of 370 Bq.kg<sup>-1</sup>, as delineated in [24].

#### G. External Hazard Index $H_{ex}$

The External Hazard Index ( $H_{ex}$ ) is designed to estimate the potential radiation dose from the gamma rays emitted by building materials, assuming thick wall structures devoid of windows and doors [23]. The computation of  $H_{ex}$  values, as per the methodology outlined in [23], is crucial in assessing whether the radiation hazard posed by these materials is negligible. For the hazard to be considered insignificant, the  $H_{ex}$  values must remain below the threshold of 1.

$$H_{ex} = \frac{C_{226Ra}}{370} + \frac{C_{232Th}}{259} + \frac{C_{40K}}{4810} . \quad (6)$$

#### H. Internal Hazard Index $H_{in}$

The Internal Hazard Index ( $H_{in}$ ) quantifies the internal exposure to radon and its progeny, complementing the External Hazard Index ( $H_{ex}$ ) assessment. As articulated in [24], to effectively mitigate the risks associated with <sup>226</sup>Ra, it is necessary to reduce its maximum permissible concentration to half of the standard limit, equating to 185 Bq.kg<sup>-1</sup>.

$$H_{in} = \frac{C_{226Ra}}{185} + \frac{C_{232Th}}{259} + \frac{C_{40K}}{4810} . \quad (7)$$

It is essential to maintain the values of this index below 1 to ascertain that the associated radiation risks are considered negligible.

#### I. Absorbed gamma dose rate

The calculation of the absorbed gamma dose rate, arising from the emissions of radionuclides (<sup>226</sup>Ra, <sup>232</sup>Th, and <sup>40</sup>K) and Naturally Occurring Radioactive Materials (NORMs) in building materials, was performed employing the methodologies outlined in the European Commission Report [25, 26]. The formula for this calculation is as follows:

$$D_R (nGy.h^{-1}) = 0.92C_{Ra} + 1.1C_{Th} + 0.08C_K . \quad (8)$$

The global average for the Absorbed dose rate is documented to be 55 nGy.h<sup>-1</sup> [27].

#### J. Annual effective doses rate (AED)

The computation of the Annual Effective Dose (AED) indoors considers a conversion coefficient, transforming the absorbed dose rate in the air ( $D_R$ ) into an annual effective dose. This coefficient is quantified at 0.7 Sv.Gy<sup>-1</sup>. The calculation further incorporates an indoor occupancy factor of 0.8, indicative of the average condition where individuals spend about 80% of their time indoors. Additionally, ' $T$ ' represents the total number of hours a year, quantified as 8760 h y<sup>-1</sup>, per the guidelines in [28].

$$AED(mSv.y^{-1}) = D_R \times T \times 0.8 \times 0.7 \times 10^{-6} . \quad (9)$$

### III. RESULTS

#### *Testing of sealing methods for cylindrical plastic containers used in gamma spectrometry measurements*

In order to evaluate radon leakage from cylindrical plastic containers, radon concentration was monitored within an acrylate accumulation chamber over 15 days, with data acquisition occurring every 15 minutes. The average background radon concentration within this chamber was recorded as  $(13.4 \pm 10.2) \text{ Bq.m}^{-3}$  (mean  $\pm$  standard deviation).

Results presented in Figure 5 reveal that the radon concentration for the initial sealing method was markedly higher, approximately 97 times greater than the average background radon concentration, indicating its inefficiency. While demonstrating reduced leakage, the second method still registered radon levels about 15 times above the background concentration. In contrast, the final method, incorporating Teflon tape and high-vacuum grease, displayed near-perfect hermetic sealing, signifying negligible leakage. The average radon concentration for this method was  $(17.9 \pm 9.5) \text{ Bq.m}^{-3}$ , statistically on par with the background radon concentration. This finding underscores the efficacy of the third sealing method in ensuring the air-tightness of the containers, a critical factor in numerous studies focused on measuring  $^{226}\text{Ra}$  activity through gamma-ray spectrometry of natural samples [29-31].

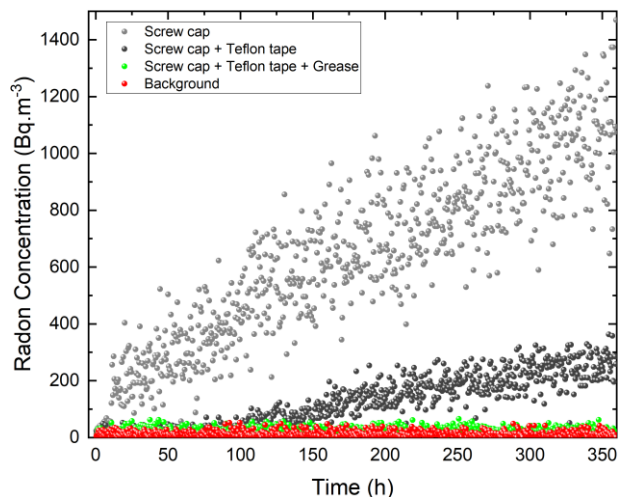


Fig. 5 Comparison of the time evolution of radon leakage for the three sealing methods vs. background concentration for the plastic cylindrical containers.

#### *Activity concentrations of $^{226}\text{Ra}$ , $^{232}\text{Th}$ , and $^{40}\text{K}$*

The Minimum Detectable Activity (MDA) was established at  $6.6 \text{ Bq.kg}^{-1}$  for  $^{226}\text{Ra}$ ,  $6.2 \text{ Bq.kg}^{-1}$  for  $^{232}\text{Th}$ , and  $32 \text{ Bq.kg}^{-1}$  for  $^{40}\text{K}$ . Table 1 delineates the activity concentrations of  $^{226}\text{Ra}$ ,  $^{232}\text{Th}$ , and  $^{40}\text{K}$ , expressed in  $\text{Bq.kg}^{-1}$ . The concentrations of  $^{226}\text{Ra}$  ranged from below the detection limit (BDL) to  $60.6 \text{ Bq.kg}^{-1}$ , averaging  $39.4 \text{ Bq.kg}^{-1}$ . The

$^{232}\text{Th}$  concentrations varied from BDL to  $22.3 \text{ Bq.kg}^{-1}$ , with a mean of  $13 \text{ Bq.kg}^{-1}$ . The  $^{40}\text{K}$  levels spanned from BDL to  $1074 \text{ Bq.kg}^{-1}$ , with an average of  $702 \text{ Bq.kg}^{-1}$ .

According to UNSCEAR [28], the global average activity levels for  $^{226}\text{Ra}$ ,  $^{232}\text{Th}$ , and  $^{40}\text{K}$  are  $35 \text{ Bq.kg}^{-1}$ ,  $30 \text{ Bq.kg}^{-1}$ , and  $400 \text{ Bq.kg}^{-1}$ , respectively. The Cement PR, Cement PV, Sand G, Sand F2, Concrete, and brick samples exhibited  $^{226}\text{Ra}$  values marginally exceeding the global average. Only Cement A and Cement PV recorded  $^{40}\text{K}$  values below the global average. In contrast, the  $^{232}\text{Th}$  concentration in all samples consistently remained below the global average.

Gypsum samples exhibited the lowest levels of all primary radionuclides, whereas the brick samples had the highest levels of  $^{226}\text{Ra}$  ( $60.6 \text{ Bq.kg}^{-1}$ ),  $^{232}\text{Th}$  ( $22.3 \text{ Bq.kg}^{-1}$ ), and  $^{40}\text{K}$  ( $1074 \text{ Bq.kg}^{-1}$ ).

Table 1: Concentration of radioactivity for  $^{226}\text{Ra}$ ,  $^{232}\text{Th}$ , and  $^{40}\text{K}$  in powdered building material samples from the Central Coast of Peru. BDL: Below the detection limit. \*The letters accompanying the construction materials indicate the brands of these products.

| Samples Building Materials * |           | Activity Concentration ( $\text{Bq.kg}^{-1}$ ) |                   |                   |
|------------------------------|-----------|--|-------------------|-------------------|
|                              |           | $^{40}\text{K}$                                | $^{226}\text{Ra}$ | $^{232}\text{Th}$ |
| 1                            | Cement S  | 405 $\pm$ 19                                   | 33.3 $\pm$ 1.0    | 7.8 $\pm$ 0.8     |
| 2                            | Cement PR | 579 $\pm$ 27                                   | 42.5 $\pm$ 1.6    | 10.8 $\pm$ 1.0    |
| 3                            | Cement A  | 347 $\pm$ 16                                   | 31.8 $\pm$ 1.2    | 7.8 $\pm$ 0.8     |
| 4                            | Cement PV | 356 $\pm$ 17                                   | 43.8 $\pm$ 1.7    | 9.9 $\pm$ 1.0     |
| 5                            | Cement Y  | 821 $\pm$ 39                                   | 30.0 $\pm$ 1.1    | 9.5 $\pm$ 0.9     |
| 6                            | Sand G    | 924 $\pm$ 44                                   | 40.9 $\pm$ 1.5    | 15.4 $\pm$ 1.5    |
| 7                            | Sand F1   | 898 $\pm$ 43                                   | 23.8 $\pm$ 0.9    | 7.7 $\pm$ 0.7     |
| 8                            | Sand F2   | 834 $\pm$ 40                                   | 42.1 $\pm$ 1.6    | 13.4 $\pm$ 1.3    |
| 9                            | Gypsum M  | BDL  | BDL               | BDL               |
| 10                           | Gypsum L  | BDL  | BDL               | BDL               |
| 11                           | Concrete  | 667 $\pm$ 33                                   | 44.4 $\pm$ 1.7    | 19.6 $\pm$ 1.9    |
| 12                           | Rock      | 452 $\pm$ 21                                   | 28.7 $\pm$ 1.1    | 10.8 $\pm$ 1.0    |
| 13                           | Brick P8  | 1067 $\pm$ 51                                  | 60.6 $\pm$ 2.3    | 21.4 $\pm$ 2.1    |
| 14                           | Brick P9  | 1074 $\pm$ 51                                  | 50.6 $\pm$ 1.9    | 22.3 $\pm$ 2.2    |

#### *Radon mass exhalation rate and Radon emanation fraction*

Table 2 comprehensively presents the radon mass exhalation rates for all samples, encapsulating the slope "m" that signifies the linear increase in radon concentration during the initial 24-hour measurement period, along with the radon emanation fraction f. A robust correlation was observed between the total radium content and the radon mass exhalation rate in cement samples, as depicted in Figure 6 ( $R^2=0.99$ ). The radon mass exhalation rate (EM) ranged from  $(4.50 \pm 0.42) \text{ mBq.kg}^{-1}.\text{h}^{-1}$  to  $(22.34 \pm 1.30) \text{ mBq.kg}^{-1}.\text{h}^{-1}$ , averaging  $(14.01 \pm 1.04) \text{ mBq.kg}^{-1}.\text{h}^{-1}$ . The average radon mass exhalation rates for Cement and Gypsum samples aligned with values reported in [32]. Brick samples exhibited a higher radon exhalation rate than other materials. Gypsum samples showed minimal radon

exhalation, correlating with their lower radium content. The radon emanation fraction for each building material was calculated using Equation (3), with average values of 5.9% for cement, 8.6% for sand, 7.1% for concrete, 5.1% for rock, and 11.6% for bricks. Figure 6 illustrates a strong positive correlation (0.99) between radium activity concentration and radon exhalation rate in cement samples, underscoring the significant relationship between these parameters.

Table 2: The Radon mass exhalation rate ( $E_M$ ), the initial slope of radon concentration increase ( $m$ ) in the accumulation chamber, and the radon emanation fraction ( $f$ ) of the building material samples.

| Samples    | $m$ ( $Bq \cdot m^{-3} \cdot h^{-1}$ ) | $E_M$ ( $mBq \cdot kg^{-1} \cdot h^{-1}$ ) | $f$ (%) |
|------------|--|--|---------|
| Cement S   | 0.98±0.07                              | 13.1±0.9                                   | 5.2     |
| Cement PR  | 1.77±0.06                              | 20.8±1.4                                   | 6.5     |
| Cement A   | 1.30±0.07                              | 14.5±1.1                                   | 6.0     |
| Cement PV  | 1.34±0.07                              | 21.0±1.3                                   | 6.4     |
| Cement Y   | 0.93±0.08                              | 12.9±1.1                                   | 5.7     |
| Sand G     | 2.40±0.07                              | 29.8±1.8                                   | 9.6     |
| Sand F1    | 1.44±0.08                              | 13.7±1.1                                   | 7.6     |
| Sand F2    | 1.04±0.07                              | 18.8±1.1                                   | 5.9     |
| Gypsum M   | 0.21±0.09                              | BDL  | BDL     |
| Gypsum L   | 0.25±0.09                              | BDL  | BDL     |
| Concrete 1 | 1.75±0.07                              | 23.9±1.5                                   | 7.1     |
| Rock C     | 1.15±0.08                              | 11.1±0.9                                   | 5.1     |
| Brick P8   | 2.45±0.05                              | 52.3±2.4                                   | 13.6    |
| Brick P9   | 1.25±0.06                              | 44.2±2.1                                   | 11.6    |

#### Radiological parameters

Table 3 summarizes the range and mean  $\pm$  standard deviation (SD) values for key radiological parameters: Gamma Index ( $I_\gamma$ ), Radium Equivalent ( $Ra_{eq}$ ), External Hazard Index ( $H_{ex}$ ), Internal Hazard Index ( $H_{in}$ ), Absorbed Gamma Dose Rate (DR), and Annual Effective Dose (AED). Building materials such as Cement, Sand, Concrete, and Gypsum exhibited a gamma index of  $\leq 0.5$ , aligning with the exemption dose criterion of

0.3  $mSv \cdot y^{-1}$ . The latter indicates that these materials are classified as exempt and are suitable for unrestricted use. Conversely, the  $I_\gamma$  values for brick samples surpass this exemption criterion yet comply with the  $I_\gamma \leq 1$  criterion. This compliance signifies that their usage does not exceed 1  $mSv \cdot y^{-1}$  limit, rendering them acceptable for building construction.

Regarding  $Ra_{eq}$ , all samples are deemed safe from a radiological protection perspective, as they register values below  $370 Bq \cdot kg^{-1}$ , by [33]. The calculated values for the External Hazard Index ( $H_{ex}$ ) and Internal Hazard Index ( $H_{in}$ ) were less than 1 for all evaluated building materials, ensuring a minimal radiation risk associated with their use. Only the brick samples exceeded the dose level of  $55 nGy \cdot h^{-1}$  among the analyzed samples. However, the annual effective doses remained below the recommended limit of  $1 mSv \cdot y^{-1}$ , as suggested by [34].

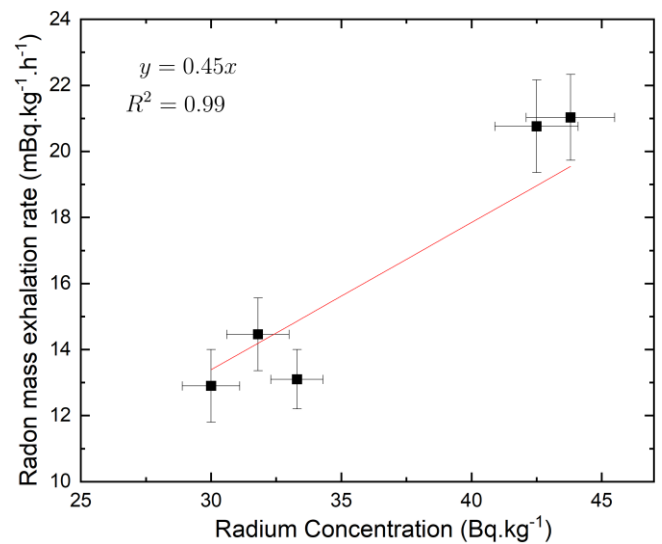


Fig. 6 Correlation between Radon mass exhalation rate and Radium concentration of cement samples.

#### IV. CONCLUSIONS

This research thoroughly evaluates the efficacy of different sealing techniques applied to cylindrical plastic containers used in gamma spectrometry. Among the methods tested, the combined application of Teflon tape and high-vacuum grease has emerged as the most effective, as demonstrated by its adherence to the minimum detectable concentration (MDC) criteria, established at  $44 Bq \cdot m^{-3}$ . This innovative sealing approach is particularly adept at preserving the container's airtightness, a critical factor for maintaining the secular equilibrium between  $^{226}Ra$  and its radon progeny. Achieving this equilibrium is essential for indirectly determining the radium content in the samples.

Table 3: Average of the different radiological hazard indices for the analysed building

| Building material | No | $I_\gamma$ | $Ra_{eq}$ (Bq.kg <sup>-1</sup> ) | $H_{ex}$  | $H_{in}$  | D (nGy.h <sup>-1</sup> ) | AED (μSv.y <sup>-1</sup> ) |
|-------------------|----|------------|----------------------------------|-----------|-----------|--------------------------|----------------------------|
| Cement            | 5  | 0.33±0.07  | 36.28±6.40                       | 0.24±0.04 | 0.34±0.05 | 43.21±8.57               | 0.21±0.04                  |
| Sand              | 3  | 0.47±0.05  | 35.60±10.24                      | 0.33±0.04 | 0.42±0.07 | 60.71±6.96               | 0.30±0.03                  |
| Gypsum            | -  | -          | -                                | -         | -         | -                        | -                          |
| Concrete          | 1  | 0.52       | 60                               | 0.38      | 0.54      | 67.37                    | 0.33                       |
| Rock              | 1  | 0.30       | 28.7                             | 0.21      | 0.29      | 38.63                    | 0.19                       |
| Brick             | 2  | 0.65±0.02  | 51.00±7.07                       | 0.46±0.02 | 0.61±0.03 | 83±2.68                  | 0.41±0.01                  |

In gamma spectrometry, the precision of sealing methods holds significant importance, especially when measuring natural radioactivity in Naturally Occurring Radioactive Material (NORM) and Technically Enhanced Naturally Occurring Radioactive Material (TENORM). The effectiveness of the seal directly influences the accuracy and dependability of these radioactivity measurements. Consequently, the findings of this study play a crucial role in informing optimal practices in gamma spectrometry, thereby enhancing the precision of radioactivity assessments in various materials. This advancement contributes to the more reliable and safe handling of radioactive substances across research and industrial spheres.

The analytical assessment of primary radioisotopes, notably <sup>226</sup>Ra, <sup>232</sup>Th, and <sup>40</sup>K, in various materials yielded insightful results concerning their concentration levels. The detected <sup>226</sup>Ra content was generally aligned with or marginally surpassed the global average. In contrast, the <sup>232</sup>Th levels did not exceed the global mean in any of the analyzed samples, while <sup>40</sup>K exceeded this average in two instances. Regarding radiological risk assessment, utilizing indices such as the Gamma index ( $I_\gamma$ ), only brick samples exceeded the exemption threshold of 0.3 mSv.y<sup>-1</sup> yet remained below the more stringent limit of 1 mSv.y<sup>-1</sup>. This trend was observed across other criteria, including the Radium Equivalent ( $Ra_{eq}$ ), External Hazard Index ( $H_{ex}$ ), and Internal Hazard Index ( $H_{in}$ ).

Furthermore, gamma dose rate calculations revealed that Sand, Concrete, and Brick presented levels above the global average of 55 nGy.h<sup>-1</sup> but still fell within the recommended limits set by UNSCEAR. The latter could be attributed to the geographical proximity of raw material extraction sites for brick production to uranium-rich regions. Significantly, the study identified a strong correlation between radon mass exhalation and radon exhalation rates in cement samples, indicating a homogenous distribution of <sup>226</sup>Ra in the cement's raw material sources.

Based on the evaluated radiological indices – Radium Equivalent ( $Ra_{eq}$ ), Gamma Index ( $I_\gamma$ ), External Hazard Index ( $H_{ex}$ ), and Internal Hazard Index ( $H_{in}$ ) – all investigated building materials are deemed safe for use. The values for these radiological indices were all below the thresholds recommended by UNSCEAR. The insights from this research are fundamental in establishing national guidelines in Peru aimed at regulating radiation exposure from building materials, ensuring public safety, and aligning with international standards. Hence, this study bears significant implications for public health and safety regulations in the construction sector.

#### ACKNOWLEDGMENT

This study was carried out as part of the project CAP 2018-3-0018/ PI 578, the National Council of Science, Technology and Technological Innovation (CONCYTEC) under the PhD scholarship program (236-2015-FONDECYT) and Universidad Señor de Sipán with Resolution N° 079-2022 - N°11. The authors thank the GITHUNU-PUCP team.

#### REFERENCES

- [1] R. G. Sonkawade, K. Kant, S. Muralithar, R. Kumar, and R. C. Ramola, "Natural radioactivity in common building construction and radiation shielding materials," *Atmospheric Environment*, vol. 42, no. 9, pp. 2254–2259, Mar. 2008, doi: <https://doi.org/10.1016/j.atmosenv.2007.11.037>.
- [2] J-F. Lecomte, "ICRP Publication 142: Radiological Protection from Naturally Occurring Radioactive Material (NORM) in Industrial Processes - J-F. Lecomte, P. Shaw, A. Liland, M. Markkanen, P. Egidii, S. Andresz, J. Mrdakovic-Popic, F. Liu, D. da Costa Lauria, H.B. Okyar, P.P. Haridasan, S. Mundigl, 2019," *Annals of the ICRP*, 2019. <https://journals.sagepub.com/doi/10.1177/0146645319874589> (accessed Jan. 23, 2024).
- [3] R. C. Ramola, G. S. Gusain, M. Badoni, Y. Prasad, G. Prasad, and T. V. Ramachandran, "226Ra, 232Th and 40K contents in soil samples from Garhwal Himalaya, India, and its radiological implications," *Journal of Radiological Protection*, vol. 28, no. 3, pp. 379–385, Aug. 2008, doi: <https://doi.org/10.1088/0952-4746/28/3/008>.
- [4] C. Coletti et al., "Radionuclide concentration and radon exhalation in new mix design of bricks produced reusing NORM by-products: The influence of mineralogy and texture," *Construction and Building Materials*, vol.

- 260, pp. 119820–119820, Nov. 2020, doi: <https://doi.org/10.1016/j.conbuildmat.2020.119820>.
- [5] Leonel, António Curado, Luís Graça, S. Soares, and Sérgio Ivan Lopes, “Impacts of Indoor Radon on Health: A Comprehensive Review on Causes, Assessment and Remediation Strategies,” *International Journal of Environmental Research and Public Health*, vol. 19, no. 7, pp. 3929–3929, Mar. 2022, doi: <https://doi.org/10.3390/ijerph19073929>.
- [6] D. B. Chambers, “Thoron and decay products, beyond UNSCEAR 2006 Annex E,” *Radiation Protection Dosimetry*, vol. 141, no. 4, pp. 351–356, Oct. 2010, doi: <https://doi.org/10.1093/rpd/ncq224>.
- [7] D. Jasaitis and M. Pečiulienė, “Natural Radioactivity and Radon Exhalation from Building Materials in Underground Parking Lots,” *Applied sciences*, vol. 11, no. 16, pp. 7475–7475, Aug. 2021, doi: <https://doi.org/10.3390/app11167475>.
- [8] Y. Omori et al., “Radiation dose due to radon and thoron progeny inhalation in high-level natural radiation areas of Kerala, India,” *Journal of Radiological Protection*, vol. 37, no. 1, pp. 111–126, Dec. 2016, doi: <https://doi.org/10.1088/1361-6498/37/1/111>.
- [9] Y. Ishimori, K. Lange, P. Martin, Y. Mayya, and M. Phaneuf, “Measurement and Calculation of Radon Releases from NORM Residues.” Available: [https://www-pub.iaea.org/MTCD/Publications/PDF/trs474\\_webfile.pdf](https://www-pub.iaea.org/MTCD/Publications/PDF/trs474_webfile.pdf)
- [10] N. M. Hassan et al., “Radon Migration Process and Its Influence Factors; Review,” *Japanese Journal of Health Physics*, vol. 44, no. 2, pp. 218–231, Jan. 2009, doi: <https://doi.org/10.5453/jhps.44.218>.
- [11] P. Pereyra et al., “Estimation of Indoor <sup>222</sup>Rn Concentration in Lima, Peru Using LR-115 Nuclear Track Detectors Exposed in Different Modes,” *Atmosphere*, vol. 14, no. 6, pp. 952–952, May 2023, doi: <https://doi.org/10.3390/atmos14060952>.
- [12] R. Liza, P. Pereyra, J. Rau, M. Guzmán, L. Sajó-Bohus, and D. Palacios, “Assessment of Natural Radioactivity and Radon Exhalation in Peruvian Gold Mine Tailings to Produce a Geopolymer Cement,” *Atmosphere*, vol. 14, no. 3, pp. 588–588, Mar. 2023, doi: <https://doi.org/10.3390/atmos14030588>.
- [13] Rivera, R. Realidad y Perspectivas de los Minerales Radioactivos en el Perú. INGEMMET, 2010
- [14] J. M. Stajić and D. Nikezić, “Measurement of radon exhalation rates from some building materials used in Serbian construction,” *Journal of Radioanalytical and Nuclear Chemistry*, Nov. 2014, doi: <https://doi.org/10.1007/s10967-014-3726-5>.
- [15] Konstantin Kovler, A. Perevalov, V. Steiner, and L. Metzger, “Radon exhalation of cementitious materials made with coal fly ash: Part 1 – scientific background and testing of the cement and fly ash emanation,” *Journal of Environmental Radioactivity*, vol. 82, no. 3, pp. 321–334, Jan. 2005, doi: <https://doi.org/10.1016/j.jenvrad.2005.02.004>.
- [16] I. Gutiérrez-Álvarez, J. Martín, José Antonio Adame, C. Grossi, A. Vargas, and J.P. Bolívar, “Applicability of the closed-circuit accumulation chamber technique to measure radon surface exhalation rate under laboratory conditions,” *Radiation Measurements*, vol. 133, pp. 106284–106284, Apr. 2020, doi: <https://doi.org/10.1016/j.radmeas.2020.106284>.
- [17] I. López-Coto, J. L. Mas, J. Pedro, and R. García-Tenorio, “A short-time method to measure the radon potential of porous materials,” *Applied Radiation and Isotopes*, vol. 67, no. 1, pp. 133–138, Jan. 2009, doi: <https://doi.org/10.1016/j.apradiso.2008.07.015>.
- [18] C. Cosma, A. Cucuș-Dinu, B. Papp, R. Begy, and C. Săinz, “Soil and building material as main sources of indoor radon in Băița-Ștei radon prone area (Romania),” *Journal of Environmental Radioactivity*, vol. 116, pp. 174–179, Feb. 2013, doi: <https://doi.org/10.1016/j.jenvrad.2012.09.006>.
- [19] P. Tuccimei, M. Castelluccio, M. Soligo, and M. Moroni, “RADON EXHALATION RATES OF BUILDING MATERIALS: EXPERIMENTAL, ANALYTICAL PROTOCOL AND CLASSIFICATION CRITERIA.” Accessed: Jan. 24, 2024. [Online]. Available: <https://www.radon.it/site/download/Protocol-ExhalationRates.pdf>
- [20] S. Righi and L. Bruzzi, “Natural radioactivity and radon exhalation in building materials used in Italian dwellings,” *Journal of Environmental Radioactivity*, vol. 88, no. 2, pp. 158–170, Jan. 2006, doi: <https://doi.org/10.1016/j.jenvrad.2006.01.009>.
- [21] “European Commission (EC) (1999) Radiation protection 112. Radiological Protection Principles Concerning the Natural Radioactivity of Building Materials, Directorate General Environment, Nuclear Safety and Civil Protection. - References - Scientific Research Publishing,” Scirp.org, 2014. <https://www.scirp.org/reference/ReferencesPapers?ReferenceID=1077862> (accessed Jan. 24, 2024).
- [22] Mayeen Uddin Khandaker, P. J. Jojo, Hasan Abu Kassim, and Yusoff Mohd Amin, “Radiometric analysis of construction materials using HPGe gamma-ray spectrometry,” *Radiation Protection Dosimetry*, vol. 152, no. 1–3, pp. 33–37, Aug. 2012, doi: <https://doi.org/10.1093/rpd/ncs145>.
- [23] Beretka, J.; Mathew, P., “Natural Radioactivity of Australian Building Materials,” *Health Physics*, LWV, 2024. [https://journals.lww.com/health-physics/abstract/1985/01000/natural\\_radioactivity\\_of\\_australian\\_building.7.aspx](https://journals.lww.com/health-physics/abstract/1985/01000/natural_radioactivity_of_australian_building.7.aspx).
- [24] Raghu, Y.; Ravisankar, R.; Chandrasekaran, A.; Vijayagopal, P.; Venkatraman, B. Assessment of natural radioactivity and 354, radiological hazards in building materials used in the Tiruvannamalai District, Tamilnadu, India, using a statistical approach. 355, *Journal of Taibah University for Science* 2017, 11, 523–533. <https://doi.org/10.1016/j.jtusc.2015.08.004>.
- [25] Commission, E.E.; et al. Radiological protection principles concerning the natural radioactivity of building materials. *Radiation 357 Protection* 1999, 112.
- [26] Othman, S.Q.; Ahmed, A.H.; Mohammed, S.I. Natural radioactivity and radiological risk assessment due to building materials 359 commonly used in Erbil city, Kurdistan region, Iraq. *Environmental Monitoring and Assessment* 2023, 195, 140.
- [27] UNSCEAR. Sources and Effects of Ionizing Radiation, United Nations Scientific Committee on the Effects of Atomic Radiation; 361 United Nations Publication, New York, 2008.
- [28] UNSCEAR. Sources and effects of Ionizing Radiation. United Nations, New York 2000.
- [29] J. Scholten, I. Osvath, and Mai Khanh Pham, “<sup>226</sup>Ra measurements through gamma spectrometric counting of radon progenies: How significant is the loss of radon?,” *Marine Chemistry*, vol. 156, pp. 146–152, Oct. 2013, doi: <https://doi.org/10.1016/j.marchem.2013.03.001>.
- [30] M. Bonczyk and Krzysztof Samolej, “Testing of the radon tightness of beakers and different types of sealing used in gamma-ray spectrometry for <sup>226</sup>Ra concentration determination in NORM,” *Journal of Environmental Radioactivity*, vol. 205–206, pp. 55–60, Sep. 2019, doi: <https://doi.org/10.1016/j.jenvrad.2019.05.007>.
- [31] Nur Syamsi Syam, S. Lim, Hae Young Lee, and Sang Hoon Lee, “Determination of radon leakage from sample container for gamma spectrometry measurement of <sup>226</sup>Ra,” *Journal of Environmental Radioactivity*, vol. 220–221, pp. 106275–106275, Sep. 2020, doi: <https://doi.org/10.1016/j.jenvrad.2020.106275>.
- [32] S. Frutos-Puerto, Eduardo Pinilla Gil, E. Thome, M. Reis, M. J. Madruga, and Conrado Miró Rodríguez, “Radon and thoron exhalation rate, emanation factor and radioactivity risks of building materials of the Iberian Peninsula,” *PeerJ*, vol. 8, pp. e10331–e10331, Nov. 2020, doi: <https://doi.org/10.7717/peerj.10331>.
- [33] Schroevers, W, “Naturally Occurring Radioactive Materials in Construction,” Elsevier eBooks, Jan. 2017, doi: <https://doi.org/10.1016/c2016-0-00665-4>.
- [34] Valentin, J.; et al. The 2007 recommendations of the international commission on radiological protection; Vol. 37, Elsevier Oxford, 3762007. <https://doi.org/10.1016/j.icrp.2007.10.003>. 377